SLAC-PUB-3947
LBL-21503
May 1986
(T/E)

MEASUREMENT OF THE D^0 AND D^+ LIFETIMES*

L. Gladney[a], J. A. Jaros, R. A. Ong, G. S. Abrams, D. Amidei[b], A. R. Baden, T. Barklow, A. M. Boyarski, J. Boyer, M. Breidenbach, P. Burchat[c], D. L. Burke, F. Butler, J. M. Dorfan, G. J. Feldman, G. Gidal, M. S. Gold, G. Goldhaber, L. Golding[d], J. Haggerty, G. Hanson, K. Hayes, D. Herrup, R. J. Hollebeek, W. R. Innes, I. Juricic, J. A. Kadyk, D. Karlen, A. J. Lankford, R. R. Larsen, B. W. LeClaire, M. E. Levi, N. S. Lockyer[a], V. Lüth, C. Matteuzzi[e] M. E. Nelson[f], M. L. Perl, B. Richter, K. Riles, M. C. Ross, P. C. Rowson[g], T. Schaad[h], H. Schellman[b], W. B. Schmidke, P. D. Sheldon, G. H. Trilling, C. de la Vaissiere[i], D. R. Wood, J. M. Yelton[j], and C. Zaiser

Stanford Linear Accelerator Center
Stanford University, Stanford, California 94305

Lawrence Berkeley Laboratory and Department of Physics
University of California, Berkeley, California 94720

Department of Physics
Harvard University, Cambridge, Massachusetts 02138

Submitted to *Physical Review D*

---

*This work was supported in part by the Department of Energy, contracts DE-AC03-76SF00515, DE-AC03-76SF00098, and DE-AC02-76ER03064.

[a]Present address: U. of Pennsylvania, Philadelphia, PA 19104
[b]Present address: U. of Chicago, Chicago, IL 60637
[c]Present address: U. of California, Santa Cruz, Santa Cruz CA 95064
[d]Present address: Therma Wave Corp., Fremont CA 94539
[e]Present address: CERN, CH-1211 Geneva 23, Switzerland
[f]Present address: California Insitute of Technology, Pasadena, CA 91125
[g]Present address: Columbia University, New York, NY 10027
[h]Present address: U. of Geneva, CH-1211 Geneva 4, Switzerland
[i]Present address: LPNHE, U. Pierre et Marie Curie, Paris, France F-75230
[j]Present address: Oxford University, Oxford England

ABSTRACT

We have used a high-resolution drift chamber in the Mark II Detector at PEP to measure the lifetimes of D^0 and D^+ mesons produced in e^+e^- annihilations at 29 GeV. Based on a sample of 74 decays for the D^0 mesons and 23 decays for the D^+ mesons, the lifetimes are found to be $4.7^{+0.9}_{-0.8} \pm 0.5 \times 10^{-13}$ sec and $8.9^{+3.8}_{-2.7} \pm 1.3 \times 10^{-13}$ sec, respectively. This leads to a ratio of lifetimes of $1.9^{+0.9}_{-0.7} \pm 0.3$.

I. INTRODUCTION

It has taken several years to develop techniques for making reliable measurements of charmed meson lifetimes. Since these lifetimes are on the order of 10^{-13} sec, detection devices with extremely high resolution, such as emulsions, bubble chambers, and silicon strip detectors have been used to make most of these measurements thus far.[1]

In this paper, we report on high resolution drift chamber measurements of the lifetimes of D^0 and D^+ mesons produced in e^+e^- annihilations.[2] This approach differs from measurements made by other techniques in several ways. First, since the selection of charmed particles is accomplished without regard to their decay length, the sample has essentially no bias toward long or short lifetimes. Second, since the decays are fully reconstructed, the charmed particle momenta, and hence the proper decay times, are directly measured. Third, our approach can be readily applied to τ lepton decays, which provides a good check on our technique. Finally, one disadvantage of our approach is that the error in each measurement of the decay length is comparable to the average decay length measured. Hence the statistical power per event is somewhat smaller than those of experiments with better resolution.

The data used in this analysis were collected with the Mark II detector at the PEP storage ring (29 GeV center-of-mass energy) and correspond to an integrated luminosity of 205 pb^{-1} . We have previously reported a measurement of the D^0 lifetime based on the analysis of the first 136 pb^{-1} of this data set.[3] The present analysis,[4] which includes refinements and extensions of the earlier work, supercedes it.

II. EXPERIMENTAL DETAILS

The Mark II detector at PEP has been described in detail elsewhere.[5] A high spatial resolution drift chamber, known as the vertex chamber,[6] was added to find and measure secondary vertices from the decays of short-lived particles. The vertex chamber is inside and is concentric with the inner shell of the main drift chamber. It consists of seven axial layers of drift cells grouped into two concentric bands and contained in a pressure vessel with an outer radius of 0.35 m and a length of 1.2 m. The first band consists of four layers of drift cells starting at a radius of 10.1 cm (relative to the beam line) and extending out to 12.6 cm. The second band of three layers extends from 30.4 to 32.0 cm in radius. There are a total of 825 drift cells (270 in the first band, 555 in the second band). In each cell, sense wire layers are separated from adjacent field wire layers by a distance of 4.2 mm. Sense wires are separated from adjacent field wires within a layer by 5.3 mm. Chamber wires are positioned to an accuracy of 15 μm (rms).

The average spatial resolution is 95 μm/layer which gives a position resolution for a track at the beam interaction point of $\sigma_\perp[\mu\text{m}] = \sqrt{(85)^2 + (95/\text{p})^2}$ (p in GeV/c) in the plane perpendicular to the beams. In order to minimize multiple Coulomb scattering, the inner shell of the vertex chamber is made of beryllium and serves as the beam pipe. Thus, its thickness, 0.6% of a radiation length, is the only material between the interaction point and the first position measurement. The vertex chamber and main drift chamber operate in a solenoidal magnetic field of 2.3 kG and have a combined charged particle momentum resolution of $\delta p/p = \sqrt{(0.025)^2 + (0.010p)^2}$, when tracks are not constrained to pass through the interaction point.

The resolution and azimuthal symmetry of the chamber are checked by measurements made on Bhabha scattering events. Fig. 1 shows the distribution of the separation distance between Bhabha tracks in the vicinity of the beam collision point. Since these tracks have momenta greater than 12 GeV/c, multiple Coulomb scattering contributes only a small amount to this distance. Thus, the root mean square separation distance of these tracks, 124 μm, yields an intrinsic position error of $124/\sqrt{2}$ or 88 μm for tracks extrapolated back to the vicinity of the beam. The position resolution for hadronic tracks from those events used in this analysis was found to be about 10% worse than that found for Bhabha tracks. This degradation is largely due to electronic cross-talk in the amplifiers of the vertex chamber.

The phi symmetry of the chamber's measurements is evident in Fig. 2, which shows the mean impact parameter, in the x-y plane (transverse to the beams), with respect to the beam position for Bhabha tracks as a function of azimuthal angle. The impact parameter is defined to be positive if, when looking along a

track toward the origin, the average beam position is to the right of the track, and negative if to the left. On the scale of ~ 20 μm , no angular dependence of the mean impact parameter is observed.

Lifetime measurements at e^+e^- storage rings depend on knowledge of the position of the beam-beam interaction point. The beam positions used in our analysis were determined for every two hour run by finding the position which minimized the distance of closest approach for an ensemble of well-measured tracks. With this method, we have measured the average beam position to an accuracy of 20 μm vertically and 50 μm horizontally. The beam position was found to be stable over the course of several runs.

Stability of the beam position within a run was checked by measuring the rms spread of the measurements from two Beam Position Monitors. The monitors were positioned 4.9 m on either side of the Mark II detector along the beam line and consisted of four copper pickup electrodes which protruded a small distance into the beam pipe. Each beam bunch crossing induced voltages on the electrodes. The vertical (horizontal) position of the beam relative to the monitor was determined by measuring the ratio of induced voltages on the two electrodes on the vertical (horizontal) axis. Since the component of the Mark II solenoidal field transverse to the beams was quite small outside of the detector, the beam positions measured on either side of the detector along the beam line could be used to determine the beam position at the interaction point. These beam positions were measured every four minutes during a run. The accuracy of the voltage measurements and the stability of gain calibration limited the position resolution of the monitors to ~ 50 μm. Five percent of the runs were eliminated from the data sample, because their beam position measurements had a large rms spread, indicating that the beams had moved during the run.

Measurements of decay lengths and their errors require knowledge of the horizontal and vertical beam sizes. We measure the sizes by finding the impact parameter distributions for Bhabha tracks which are within 100 mr of the vertical and horizontal axes. Fig. 3 shows the distribution of impact parameters for vertical and horizontal tracks. We find the width of the vertical Bhabha distribution to be 493 ± 16 μm. After removing the component of the width due to our tracking resolution, we get a horizontal beam size of 481 ± 18 μm. Similarly, the width of the horizontal Bhabha distribution is 113 ± 5 μm, which yields a vertical beam size of 62 ± 9 μm.

III. D^0 ANALYSIS

The sample of D^0 mesons[7] was obtained by observing the decays

$$D^{*+} \rightarrow D^0\pi^+$$
$$\hookrightarrow K^-\pi^+ \text{ or } K^-\pi^+\pi^0$$

and their charge conjugate decays. We refer to the charged pion from the D^{*+} , produced in conjunction with the D^0 , as the bachelor pion.

The D^{*+} - D^0 mass difference is just a few MeV/c^2 greater than the π^+ mass. Thus, in the laboratory frame, the relative decay angle and momenta of the D^0 and the bachelor pion are very restricted. These tight kinematical bounds make it easy to identify the decay reactions with very little background when the energy of the D^{*+} is more than 60% of the beam energy ($z > 0.6$).

All D^{*+} candidates were chosen from a sample of about 60,000 hadronic events. Hadronic events were defined as having seven or more charged tracks and a total energy in charged tracks greater than 25% of the center of mass energy. Hadronic events were also required to have an event vertex within 5 cm radius (in the plane perpendicular to the beams) of the average beam interaction point and within 10 cm of that point along the beam direction. No particle identification was attempted, except for the removal of well-identified electrons and muons. Each charged track was considered to be both a kaon and a pion in the selection described below. π^0 candidates were formed from pairs of photons identified by the liquid argon calorimeter if the energies of the photons were between 100 MeV and 4.0 GeV and the invariant masses of the pairs were between 20 MeV/c^2 and 700 MeV/c^2 . The momenta of these photons were determined from a fit which constrained the invariant masses of the pairs to the π^0 mass. Photons with energy greater than 4.0 GeV were considered to be π^0 candidates. This criterion takes into account π^0 s in which the photons from the decay were too close together to be individually distinguished in the calorimeter, or in which the decay is asymmetric and the soft photon is lost.

All oppositely charged $K\pi$ combinations with invariant mass between 1.72 GeV/c^2 and 2.00 GeV/c^2 were considered as D^0 candidates, and their momenta constrained to be products of a D^0 decay. D^0 candidates were also formed from $K\pi\pi^0$ combinations with invariant mass between 1.76 and 1.96 GeV/c^2 . (The invariant mass region chosen for the $K\pi\pi^0$ combinations differs slightly from that region for the $K\pi$ combinations in order to optimize the signal-to- background in the former mode.) Any candidate which had a χ^2 per degree of freedom greater than 5 for the kinematic constraint to the D^0 mass was eliminated from the sample. Each D^0 candidate was combined with additional charged tracks which

had charge opposite to the kaon of the D^0 , and those combinations with a small mass difference, $\Delta M_{K\pi\pi-D^0}$ or $\Delta M_{K\pi\pi^0\pi-D^0}$, and z > 0.6 were considered as D^{*+} candidates. For those events with more than one possible D^{*+} candidate, the candidate with the smallest mass difference ΔM was chosen. We checked the invariant mass distribution of the photon pairs in those $K\pi\pi^0\pi$ combinations with a mass difference less than 200 MeV/c^2 , and found its width consistent with the $15\%/\sqrt{E}$ energy resolution of the liquid argon calorimeter.

Track quality cuts were then applied to ensure that the decay point of the D^0 meson could be well-measured. To minimize the probability that the K or π tracks from the D^0 had been scattered or mis-measured, we required that these tracks have momenta greater than 500 MeV/c and that none of the vertex chamber measurement points be shared with nearby tracks in the event. The three charged tracks from the D^{*+} were each required to contain at least three measurements in the vertex chamber, of which at least one was required to be in the inner band of drift cells. We also demanded that each track fit have an overall χ^2 per degree of freedom less than 5, and that the χ^2 per degree of freedom in the vertex chamber alone be less than 5.

A decay vertex was formed for each candidate from the two charged tracks from the D^0 decay. We then used the procedure described in Section IV to calculate the decay length and its corresponding error. We checked that each decay was consistent with the hypothesis that it originated in the vicinity of the beam interaction point by requiring that the distance of closest approach of the D^0 flight trajectory to the beam position be less than three standard deviations in the transverse error on the trajectory. The transverse error included contributions from the vertex position error and the beam size. The transverse error contribution coming from the uncertainty in the D^0 momentum direction is negligibly small in comparison to the vertex error and beam size.

Since we can obtain a good estimate of the production point of the D^{*+} from the beam and D^0 vertex information, it is possible to discriminate against events in which the low momentum bachelor pion has scattered or been mis-measured by constraining it and the virtual D^0 track to the estimated production point. We required the χ^2 per degree of freedom of this vertex fit to be less than 5. This technique improves the momentum determination of the bachelor pion and permits us to re-determine the mass difference. The mass difference after all cuts is shown in Fig. 4 for the $D^0 \rightarrow K\pi$ and $D^0 \rightarrow K\pi\pi^0$ events. D^{*+} events were defined to be those with a mass difference between 143 and 149 MeV/c^2 . In the D^{*+} region, we have a total of 39 events from the $K\pi$ mode and 35 events from the $K\pi\pi^0$ mode.

The decay lengths from the 2-particle vertices of the 74 events in Fig. 4 were used in determining the mean lifetime of the D^0 . From Fig. 4, the combinatorial

hadronic background is estimated to be $12 \pm 6\%$ for events from the $K\pi$ decay mode and $14 \pm 6\%$ for events from the $K\pi\pi$ decay mode. In the standard model, B meson decays may contribute up to 20% of the produced D^{*+} events, but phase space considerations ensure that most of these D^{*+} events are of low momentum, whereas the charm fragmentation function is known to be hard.[8] It is estimated that $3 \pm 2\%$ of the D^{*+} events with $z > 0.6$ originate from B decays.[9]

IV. PATH LENGTH MEASUREMENT

After isolating a clean sample of D mesons which we wish to study, we use information from the decay tracks to estimate the decay vertex position. We determine the path length using the technique described in our measurement on the τ lifetime.[10] Since the vertex chamber can only contribute position information in the x-y plane (the main drift chamber contributes track curvature and z position information), these vertex positions and their corresponding decay lengths relative to the known beam position are estimated only in the x-y plane. If we assume that the production point of each D meson is close to the beam interaction point, that its direction is is known perfectly, and that the errors in the estimated vertex and beam position are Gaussian, then it can be shown that the best estimate of the projected decay length is

$$\ell' = \frac{x_V B_{xx} t_x + y_V B_{yy} t_y + B_{xy}(x_V t_y + y_V t_x)}{B_{xx} t_x^2 + B_{yy} t_y^2 + 2 B_{xy} t_x t_y} \ . \tag{1}$$

where x_V, y_V is the vertex position relative to the beam position, (t_x, t_y) are the direction cosines of the particle's trajectory in the x-y plane, and B_{xx}, B_{yy}, and B_{xy} are the elements of the inverse of the error matrix formed by adding the vertex position and beam position error matrices. The error matrix associated with the beam position consists simply of the beam size in x and y. The error on the decay length is

$$\sigma_{\ell'} = \left[B_{xx} t_x^2 + B_{yy} t_y^2 + 2 B_{xy} t_x t_y \right]^{-\frac{1}{2}} \ . \tag{2}$$

The full 3-dimensional decay length is derived from the formula,

$$\ell = \frac{\ell'}{\sin\theta_D} \ . \tag{3}$$

where θ_D is the angle between the D flight path and the beam line. The decay length is converted into a proper decay time using the measured momentum of the particle. The contribution to the decay time error due to the error in determining the D momentum is negligible in comparison to the contribution due to the D vertex position determination.

V. FITTING FUNCTION

The distributions of decay lengths and proper decay times for events from both modes are shown in Fig. 5 and Fig. 6. The errors on the decay times are shown in Fig. 7. The errors for the $K\pi\pi^0$ mode are slightly larger than those for the $K\pi$ mode because the additional π^0 in the $K\pi\pi^0$ mode causes the angle between the K and π from the D^0 to decrease. This effect increases the error in the decay position of the D^0 , increasing the overall decay length error. Since the measurement errors and backgrounds of the two samples are comparable, we have combined them. Fig. 8 shows the lifetime distribution of the combined sample.

The best estimate of the mean decay time of the sample was found by a maximum likelihood fit of the proper decay times to a fitting function whose form is determined primarily by the expected exponential decay time distribution convoluted with Gaussian errors specific to each event. The fit included effects due to B meson decays and the combinatorial hadronic background. The explicit form of the logarithm of the likelihood function is

$$\ln \mathcal{L} = \sum_{i=1}^{N} \ln\Big[(1 - B_H - B_B)F_i(t) + B_H H_i(t) + B_B G_i(t)\Big] \ . \tag{4}$$

where B_H and B_B are the fractions of combinatoric background and background D^{*+} mesons from B hadron decays, respectively. The values of B_H and B_B for the D^0 analysis have been given at the end of Section III. N is the number of events in the sample. $F_i(t)$, $H_i(t)$, and $G_i(t)$ are the expected lifetime distributions for D^0 mesons, the combinatoric background, and the background from B hadrons, respectively. $F_i(t)$ is simply an exponential distribution convoluted with a Gaussian resolution for each event. Hence, letting t be the decay time, σ_t be the measured error on the decay time for each event, and τ_D be the mean D^0 lifetime,

$$\begin{aligned} F_i(t) &= \frac{1}{\sqrt{2\pi}\sigma_t \tau_D} \int_0^\infty e^{-\frac{(t-\epsilon)^2}{2\sigma_t^2}} e^{-\frac{\epsilon}{\tau_D}} d\epsilon \\ &= \frac{1}{2\tau_D}\left[e^{\left[\frac{\sigma_t^2}{2\tau_D^2} - \frac{t}{\tau_D}\right]}\left(1 - \text{ erf }\left(\frac{\sigma_t}{\sqrt{2}\tau_D} - \frac{t}{\sqrt{2}\sigma_t}\right)\right)\right]. \end{aligned} \tag{5}$$

On the basis of control samples (which are discussed in detail in Section VIII), we find that $H_i(t)$ is well-represented by a Gaussian with a mean τ_H. τ_H is greater than zero since some of the combinatoric background is presumed to contain tracks from charm and bottom decays. The exact value of the mean is determined from the data set control sample. The functional form is simply

$$H_i(t) = \frac{1}{\sqrt{2\pi}\sigma_t} e^{-\frac{(t-\tau_H)^2}{2\sigma_t^2}} \ . \tag{6}$$

We have assumed that $G_i(t)$, the function describing D^{*+} mesons produced by B decays, is formed by convoluting two exponential distributions with a Gaussian resolution function. Thus,

$$G_i(t) = \frac{1}{\sqrt{2\pi}\sigma_t(\tau_B - \tau_D)} \int_0^\infty e^{\left[-\frac{(t-\epsilon)^2}{2\sigma_t^2}\right]} \left[e^{-\frac{\epsilon}{\tau_B}} - e^{-\frac{\epsilon}{\tau_D}}\right] d\epsilon$$

$$= \frac{1}{2(\tau_B - \tau_D)} \left\{ e^{\left(\frac{\sigma_t^2}{2\tau_B^2} - \frac{t}{\tau_B}\right)} \left[1 - \text{erf}\left(\frac{\sigma_t}{\sqrt{2}\tau_B} - \frac{t}{\sqrt{2}\sigma_t}\right)\right] - \right. \tag{7}$$

$$\left. e^{\left(\frac{\sigma_t^2}{2\tau_D^2} - \frac{t}{\tau_D}\right)} \left[1 - \text{erf}\left(\frac{\sigma_t}{\sqrt{2}\tau_D} - \frac{t}{\sqrt{2}\sigma_t}\right)\right] \right\}.$$

We use as our estimate of the B lifetime,[11] $\tau_B = 10^{-12}$ sec. The results from the fit to the maximum likelihood function are shown in Fig. 6 and Fig. 8. The mean lifetimes derived from the fits for the $K\pi$ mode is 4.7×10^{-13} sec, and that for the $K\pi\pi^0$ mode is 4.8×10^{-13} sec. The measured lifetimes from the $K\pi$ and $K\pi\pi^0$ modes agree with each other quite well. We take the mean lifetime of the D^0 to be that of the combined sample of 74 events. Thus $\tau_{D^0} = 4.7^{+0.9}_{-0.8} \times 10^{-13}$ sec (statistical errors only).

VI. D^+ ANALYSIS

The analysis procedure for D^+ mesons is quite similar to that described for the D^0 . We select D^+ mesons via the decay

$$D^{*+} \rightarrow D^+\pi^0$$
$$\hookrightarrow K^-\pi^+\pi^+$$

where we can again take advantage of the low Q value of the D^{*+} decay to significantly enhance the signal to background ratio. Hadronic events and π^0 candidates were defined as described in the D^0 analysis section. Again, no particle identification was tried, all tracks were used. All $K\pi\pi$ combinations with a net charge of ± 1, where the pions have the same charge, with invariant masses between 1.68 GeV/c^2 and 2.05 GeV/c^2 were considered as D^+ candidates. Their momenta were constrained to be products of a D^+ decay. Any candidate which had a χ^2 per degree of freedom greater than 4 for the kinematic constraint to the D^+ mass was eliminated from further study. Each D^+ candidate was combined with the π^0 candidates in that event. Those combinations with a mass difference, $\Delta M_{K\pi\pi\pi^0 - D^+}$, between 0.135 and 0.200 GeV/c^2 were considered as D^{*+} candidates.

In order to ensure that the decay vertices of the D^+ candidates could be well-measured, we subjected the charged tracks in our D^+ sample to the same track quality requirements as in the D^0 analysis. A decay vertex, decay length, and decay length error were then calculated from the three charged tracks of each D^+ candidate. We required that each D^+ flight trajectory be consistent (within three standard deviations) with the hypothesis that it originated in the vicinity of the beam position.

Although selecting a clean sample of D^0 events was not difficult, we found it harder to select a clean sample of D^+ events for several reasons. First, isospin considerations demand that there be fewer D^+ decays from D^{*+} mesons than D^0 decays. Second, the π^0 from the $D^{*+} \rightarrow D^+\pi^0$ reaction has low momentum, and is often well inside a hadronic jet. Thus, our accuracy in measuring its momentum is significantly worse than our accuracy in measuring the momentum of the charged bachelor pion in the $D^{*+} \rightarrow D^0\pi^+$ decay. Third, we must deal with the increased background stemming from 3-body combinatorics when seeking D^+ decays as opposed to the 2-body combinatorics of the D^0 decays.

The ratio of bachelor π^0 energy to total D^{*+} energy must be nearly a constant for all legitimate D^{*+} events going through the D^+ π^0 decay mode. We have therefore demanded that this energy ratio for the D^{*+} candidates be between 0.045 and 0.105. The limits on this ratio are set by a Monte Carlo simulation of the $D^{*+} \rightarrow D^+\pi^0$ decay. In addition, we have eliminated multiple-counting of events (i.e. charged track combinations with several π^0 candidates) by selecting the D^{*+} candidate with the smallest χ^2 for the kinematic fit of the momenta of its photons to the π^0 mass. Fig. 9 shows the mass difference plot after all cuts for the $D^{*+} \rightarrow D^+\pi^0$ event sample. On the basis of a similar analysis on Monte Carlo events, we have chosen $135 < \Delta M_{K\pi\pi\pi^0-D^+} < 146$ MeV/c^2 as the signal region.

The signal-to-background ratio for the signal region was determined by a study of two control samples. These control samples were formed from hadronic events using the same cuts applied to the D^+ sample, with two exceptions. The first exception was the invariant mass band used to determine D^+ candidates. Fake D^+ candidates were formed from $K\pi\pi$ combinations with invariant mass between 2.05 and 2.42 MeV/c^2 for one control sample, and 1.31 and 1.67 MeV/c^2 for the other control sample. Second, tracks which combined with any other oppositely charged track in the event to form an invariant mass consistent with that of the K^0_S or Λ were rejected. Fig. 10a and Fig. 10b show the mass difference, $\Delta M_{K\pi\pi\pi^0-D^+}$ for the high and low invariant mass control samples, respectively, after all cuts.

In order to determine the amount of combinatoric background in Fig. 9, we first determined the shape of the mass difference distribution for the high and

low invariant mass control samples. We increased the statistics of these samples by eliminating the cuts on the number of vertex chamber hits, on the chi-square of the track fit, and the chi-square of the vertex fit. Cuts on tracks which overlap and on the ratio of bachelor π^0 energy to D^{*+} energy were retained. The mass difference distribution of these enlarged control samples were then fit with a trial function which had parameters controlling the shape and normalization. These parameters were allowed to vary until the best agreement with the data was obtained. Fig. 10c and 10d show the mass difference distribution for the high and low invariant mass control samples along with the best fit to the data for this function. We then fixed the parameters which controlled the shape of the function and fit the data in Fig. 10a and Fig. 10b to determine the normalization for the high and low-invariant mass control samples. The normalization for the combinatoric background in Fig. 9 was determined by interpolating between the values of the two control samples. The solid curve in Fig. 9 shows the shape of the expected combinatoric background distribution. The dotted-dashed lines show the one sigma boundaries of this curve. On the basis of a Monte Carlo study of the $D^{*+} \rightarrow D^+\pi^0$ reaction, we have determined that the excess of events outside the D^{*+} signal region is consistent with broadening of the D^{*+} mass peak due to the poor resolution on the determination of the bachelor π^0 momentum. We have used the background curve to estimate the combinatoric background from $135 < \Delta M_{K\pi\pi\pi^0-D^+} < 146$ GeV/c^2 to be 5.7 ± 3.6 events.

Using Monte Carlo techniques, we have also determined that two other backgrounds contribute to the signal. The number of D^{*+} mesons from B decays, is estimated to be $3 \pm 2\%$. Events from the decay,

$$\begin{array}{l} D^{*0} \rightarrow D^0\pi^0 \\ \qquad\quad \big\lfloor\!\!\rightarrow K^-\pi^+ \end{array}$$

in which the K and π from the D^0 are combined with a random track to make a D^+ candidate provide $14 \pm 6\%$ of the events in the signal region. The background from other charm decays is negligible.

The distribution of proper decay times for the 23 events in the signal region of Fig. 9 is shown in Fig. 11. A maximum-likelihood fit of this data using the fitting function described in Section V, which was modified to include the effects of the D^{*0} background, yields a mean D^+ lifetime of $8.9^{+3.8}_{-2.7} \times 10^{-13}$ sec (statistical errors only).

VII. CHECKS ON THE ANALYSIS

We have performed a number of checks to ensure the validity of our analysis. We have used essentially the same path length determination method in measuring the lifetime of the τ lepton.[10] This measurement is in excellent agreement with theoretical expectations and with the lifetimes determined by other experiments. We conclude that the path length measuring procedure used here is sound and essentially bias-free.

To check for biases in the vertex reconstruction and fitting procedure, we simulated D^0 and D^+ mesons produced through the D^{*+} decay mechanism using Monte Carlo techniques. In the case of the D^0 , the analysis found mean lifetimes of 0.3 ± 0.5, 2.8 ± 0.4, and $5.9 \pm 0.4 \times 10^{-13}$ sec, for input D^0 lifetimes of 0.0, 3.1, and 6.2 $\times 10^{-13}$ sec, respectively. For the D^+ simulation, the analysis yielded a lifetime of $8.4^{+1.9}_{-1.5} \times 10^{-13}$ sec for an input D^+ lifetime of 9.5×10^{-13} sec.

In order to check for any bias against long-lived events which may exist, we performed our analysis on Monte Carlo simulated events with the decay sequence $D^{*+} \rightarrow D^0\pi; D^0 \rightarrow K\pi$. The D^0 lifetime was set to 62×10^{-13} sec. We measured a mean lifetime of $59.4^{+6.0}_{-5.3} \times 10^{-13}$ sec for this sample. Thus, we have no indication of bias in measuring lifetimes from a sample with a mean lifetime about an order of magnitude higher than the measurements presented here.

VIII. SYSTEMATIC ERRORS

We have studied several sources of systematic error. The sources and magnitudes of these errors for the D^0 and D^+ analyses are summarized in Table I.

A control sample for D^0 decays was formed by selecting fake $D^0 \rightarrow K\pi$ decays out of hadronic tracks having roughly the same kinematics as real D^0 combinations. Only tracks which passed the same quality cuts applied in the D^0 and D^+ analyses were used. In order to discriminate against tracks from charm decays, we demanded that the invariant mass of the $K\pi$ combinations be between 2.05 and 2.45 GeV/c^2 . Although we did not demand that the K and π candidates have opposite charge, tracks were rejected if the invariant mass combination of the track and any other oppositely charged track in the event formed was consistent with the invariant mass of a K^0_S or Λ. The mean lifetime of the fake D^0 events was measured to be $0.6 \pm 0.3 \times 10^{-13}$ sec. A histogram of the control sample lifetimes is shown in Fig. 12. The decay time distribution for the D^+ control samples described in Section VI is shown in Fig. 13. The mean lifetime for these events is $0.8 \pm 0.5 \times 10^{-13}$ sec. We assume that the true lifetime of these control samples should be greater than zero, since there are tracks from

bottom, charm and strange decays in the sample. We confirmed this assumption by performing Monte Carlo studies as described below.

In order to verify that the Monte Carlo programs accurately simulate the data, we used the same selection criteria to find a sample of fake D^0 mesons in Monte Carlo simulated hadronic events. In this simulation, the mean bottom lifetime was set to 10^{-12} sec. The mean lifetime of the fake D^0 events from this sample was $0.5 \pm 0.2 \times 10^{-13}$ sec. We conclude that the Monte Carlo and real data control samples for the D^0 lifetime analysis agree to the level of 0.3×10^{-13} sec. Thus, we take $\pm 0.3 \times 10^{-13}$ sec as the contribution to the systematic error due to any lifetime measurement offset which may exist in the D^0 analysis. Since the D^+ control sample lifetime agrees with the result of the D^0 control sample study to the level of 0.5×10^{-13} sec, we conclude that the systematic error from any measurement offset in the D^+ analysis must be $\pm 0.5 \times 10^{-13}$ sec or less.

In the fits for the D^0 and D^+ lifetimes, the control sample lifetimes of 0.6×10^{-13} sec and 0.8×10^{-13} sec, respectively, were taken as the lifetimes of the combinatorial hadronic background. Varying the contribution of this background to the fit by the estimated one standard deviation limits for the background changes the mean lifetime of the D^0 by $\pm 0.2 \times 10^{-13}$ sec. Varying the amount of combinatoric background in the D^+ analysis within one standard deviation limits changes the mean lifetime of the D^+ by $\pm 1.1 \times 10^{-13}$ sec. As stated above, a value of 10^{-12} sec was used for the B lifetime in estimating the effect of D^{*+} mesons from B decays in the lifetime samples. Varying the contribution to the fit from this source changes the mean D^0 lifetime by $\pm 0.1 \times 10^{-13}$ sec. The effect of the uncertainty in the B background on the D^+ lifetime is $\pm 0.3 \times 10^{-13}$ sec. Since D^0 decays are a background for the D^+ analysis, we have assumed the mean lifetime of events from these decays to be 4.7×10^{-13} sec. The mean D^+ lifetime varies by $\pm 0.3 \times 10^{-13}$ sec when the amount of this background is changed from 20% to 8%. Changes in the mean D^0 lifetime of $\pm 1.0 \times 10^{-13}$ sec change the mean D^+ lifetime by $\pm 0.1 \times 10^{-13}$ sec.

The D^0 control sample was used to verify the correctness of the errors calculated by our vertexing procedure. The distribution of the ratio of the measured lifetime to the expected error for the events in the control sample is reasonably well-fit by a Gaussian of width 1.08 ± 0.06. Hence our errors in the determination of the proper decay time are larger than expected by about $8 \pm 6\%$. This is consistent with the result of a similar analysis done for our τ lifetime measurement.[10] To account for this effect, we have boosted our vertex errors by a factor of 1.08. The one sigma limits on the variation of this error change the results of the D^0 and D^+ analyses by $\pm\ 0.2 \times 10^{-13}$ sec. The measured lifetimes are insensitive to small errors in the estimated beam position and size. By adding all of the contributions in quadrature, we have determined the systematic errors on the

measurements of the D^0 and D^+ lifetimes to be 0.5×10^{-13} sec and 1.3×10^{-13} sec, respectively.

IX. CONCLUSIONS

Based on a sample of 74 D^0 decays and 23 D^+ decays we have measured lifetimes of

$$\tau_{D^0} = 4.7^{+0.9}_{-0.8} \pm 0.5 \times 10^{-13} \text{ sec and}$$
$$\tau_{D^+} = 8.9^{+3.8}_{-2.7} \pm 1.3 \times 10^{-13} \text{ sec.}$$

Assuming independent errors for the D^+ and D^0 , the ratio of lifetimes is found to be

$$\frac{\tau_{D^+}}{\tau_{D^0}} = 1.9^{+0.9}_{-0.7} \pm 0.3.$$

The current world averages[12] of the D meson lifetimes are $\tau_{D^0} = 4.29 \pm 0.53 \pm 0.42 \times 10^{-13}$ sec and $\tau_{D^+} = 9.2 \pm 1.3 \pm 1.0 \times 10^{-13}$ sec. These world averages do not include the results presented here, but do include our previous measurement .[3] The world averages yield a ratio of lifetimes of $\frac{\tau_{D^\pm}}{\tau_{D^0}} = 2.14 \pm 0.44 \pm 0.34$. Thus the results of this measurement are in good agreement with the results from other experiments.

When taken together, the measurements indicate that the lifetimes of the D^0 and D^+ are close to the theoretically predicted value for the charm quark lifetime.[13] This is a good indication that the overall properties of the hadronic decays of these mesons can be explained by the Standard Model for weak interactions.

A simple spectator model, where the lifetime of a charm meson is determined solely by the charm quark lifetime, predicts equal lifetimes for the D^0 and D^+ mesons. The difference in the D^0 and D^+ lifetimes definitely indicates that this simple model needs to be modified. The measured semileptonic branching fractions of the D^0 and D^+ mesons also indicate that the decays of the D mesons cannot be completely explained by a spectator model alone. The ratio of the semileptonic branching fractions, which should be equal to the ratio of the lifetimes given above, has most recently been measured by the Mark III collaboration.[14]

$$\frac{R(D^+ \to e^+ + X)}{R(D^0 \to e^+ + X)} = 2.3^{+0.5}_{-0.4} \pm 0.1.$$

The ratio of the semileptonic branching fractions of the D mesons agrees with the ratio of their lifetimes. That the ratio of the branching fractions is not equal to one suggests an enhancement of the D^0 nonleptonic width, or a suppression of the D^+ nonleptonic width.

ACKNOWLEDGEMENTS

We wish to thank John Butler for useful discussions on charmed meson lifetimes.

REFERENCES

1. Published measurements of charmed meson lifetimes:
E. Albini et. al., Phys. Lett. 110B, 339 (1982).
M. Aguilar-Benitez et. al., Phys. Lett. 122B, 312 (1983).
A. Badertscher et. al., Phys. Lett. 123B, 471 (1983).
M. Adamovich et. al., Phys. Lett. 140B, 119 (1984).
M. Adamovich et. al., Phys. Lett. 140B, 123 (1984).
R. Bailey et. al., Phys. Lett. 139B, 320 (1984).
M. Aguilar-Benitez et. al., Phys. Lett. 146B, 266 (1984).
R. Bailey et. al., Z. Phys. C28, 357 (1985).
M. Aguilar-Benitez et. al., CERN/EP 85-130 (1985), submitted to Z. Phys. C.
H. Yamamoto et. al., Phys. Rev. D 32, 2901 (1985).
K. Abe et. al., Phys. Rev. D D33, 1 (1986).
N. Ushida et. al., Phys Rev. Lett. 56, 1767 (1986).
N. Ushida et. al., Phys Rev. Lett. 56, 1771 (1986).
C. Jung et. al., Phys. Rev. Lett. 56, 1775 (1986).

2. Of the references given above, the papers of H. Yamamoto et. al.and C. Jung et. al.present results on the lifetimes of charmed particles produced from e^+e^- annihilation. Preliminary results on the D^0 lifetime have been presented by the HRS, TASSO, and CLEO collaborations at *International Symposium on Lepton and Photon Interactions at High Energies*, Kyoto, Japan, Aug. 19-24, 1985, edited by M. Konuma and K. Takahashi, Kyoto, Japan.

3. J. M. Yelton et. al., Phys. Rev. Lett. 52, 2019 (1984).

4. A complete discussion of this analysis may be found in
L. D. Gladney, SLAC-Report-279, (1985) Ph.D. Thesis (unpublished).

5. R. H. Schindler et. al., Phys. Rev. D24, 78 (1981).

6. J. A. Jaros, *Proceedings of the International Conference on Instrumentation for Colliding Beam Physics*, SLAC-Report 250, edited by W. Ash, Stanford, California (1982), p. 29.

7. Reference to a particle state will always imply the sum of that state and its charge conjugate state.
8. J. M. Yelton et. al., Phys. Rev. Lett. 49, 430 (1982).
9. M. E. Nelson et. al., Phys. Rev. Lett. 50, 1542 (1983).
10. J. A. Jaros et. al., Phys Rev. Lett. 51, 955 (1983).
D. Amidei, PhD. Thesis, LBL-17795 (unpublished).
11. N. Lockyer et. al., Phys. Rev. Lett. 51, 1316 (1983).
E. Fernandez et. al., Phys. Rev. Lett. 51, 1022 (1983).
12. Particle Data Group, Phys. Lett. 170B, April 10, 1986.
13. N. Cabbibo and L. Maiani, Phys. Lett. 79B, 109 (1978).
14. R. M. Baltrusaitis et. al., Phys. Rev. Lett. 54, 1976 (1985).

TABLE I. Sources and magnitudes of systematic errors.
(magnitudes in units of 10^{-13} sec.)

SOURCE	D^0	D^+
Lifetime measurement offset	± 0.3	± 0.5
Uncertainty in amount of background	± 0.2	± 1.1
Uncertainty in bottom contribution	± 0.1	± 0.3
Uncertainty in the amount of the D^0 background in the D^+ signal		± 0.3
Uncertainty in the lifetime of the D^0 background in the D^+ signal		± 0.1
Error in vertex reconstruction	± 0.2	± 0.2
Total systematic error	± 0.5	± 1.3

FIGURES

Fig. 1: Separation distance of Bhabha tracks in the vicinity of the beam position. Mean is -2.9 ± 1.2 μm; the standard deviation is 124.3 ± 3.0 μm.

Fig. 2: Mean impact parameter $< \delta >$, of Bhabha tracks as a function of azimuthal angle, ϕ.
The variation in the sizes of the error bars is due to the beam spread.

Fig. 3: Impact parameters for
a. Vertical Bhabha tracks.
Mean is -8 ± 3 μm; Standard deviation is 493 ± 15 μm.
b. Horizontal Bhabha tracks.
Mean is 9 ± 5 μm; Standard deviation is 113 ± 5 μm.

Fig. 4: Mass difference distribution after all cuts for candidates from the decay sequences
a. $D^0 \rightarrow K\pi$.
b. $D^0 \rightarrow K\pi\pi^0$.

Fig. 5: Decay length distribution after all cuts for the decays
a. $D^0 \rightarrow K\pi$.
b. $D^0 \rightarrow K\pi\pi^0$.

Fig. 6: Lifetime distribution after all cuts for the decays
a. $D^0 \rightarrow K\pi$.
b. $D^0 \rightarrow K\pi\pi^0$.
The curves show the fits to the data for lifetimes of $\tau_{D^0} = 4.7 \times 10^{-13}$ sec, and 4.8×10^{-13} sec respectively.

Fig. 7: Lifetime errors for the decays
a. $D^0 \rightarrow K\pi$.
b. $D^0 \rightarrow K\pi\pi^0$.

Fig. 8: Lifetime distribution after all cuts for the $K\pi$ and $K\pi\pi^0$ decay modes of the D^0 . The curve shows the fit to the data for a lifetime of $\tau_{D^0} = 4.7 \times 10^{-13}$ sec.

Fig. 9: Mass difference distribution after all cuts for $K\pi\pi\pi^0$ combinations with invariant mass of the $K\pi\pi$ combination between 1.68 and 2.05 $\mathrm{GeV/c^2}$.
The solid curve is the best fit to the background as described in the text.

Fig. 10: Mass difference distribution for $K\pi\pi\pi^0$ combinations after all cuts, in which the invariant mass of the $K\pi\pi$ combination lies between
a. 2.05 and 2.42 $\mathrm{GeV/c^2}$.
b. 1.31 and 1.67 $\mathrm{GeV/c^2}$.
Figures 10c and 10d are the same as 10a and 10b, respectively, except that the vertex and track quality cuts have been removed.
The solid curves are the best fits to the background data as described in the text.

Fig. 11: Lifetime distribution after all cuts for the decays $D^{*+} \rightarrow D^+\pi^0; D^+ \rightarrow K\pi\pi$.
The solid curve shows the fit to that data for a lifetime of $\tau_{D^+} = 8.9 \times 10^{-13}$ sec.

Fig. 12: Lifetime distribution for the D^0 control sample.
The mean lifetime of this distribution is $0.6 \pm 0.3 \times 10^{-13}$ sec.

Fig. 13: Lifetime distribution for the D^+ control sample.
The mean lifetime of this distribution is $0.8 \pm 0.5 \times 10^{-13}$ sec.

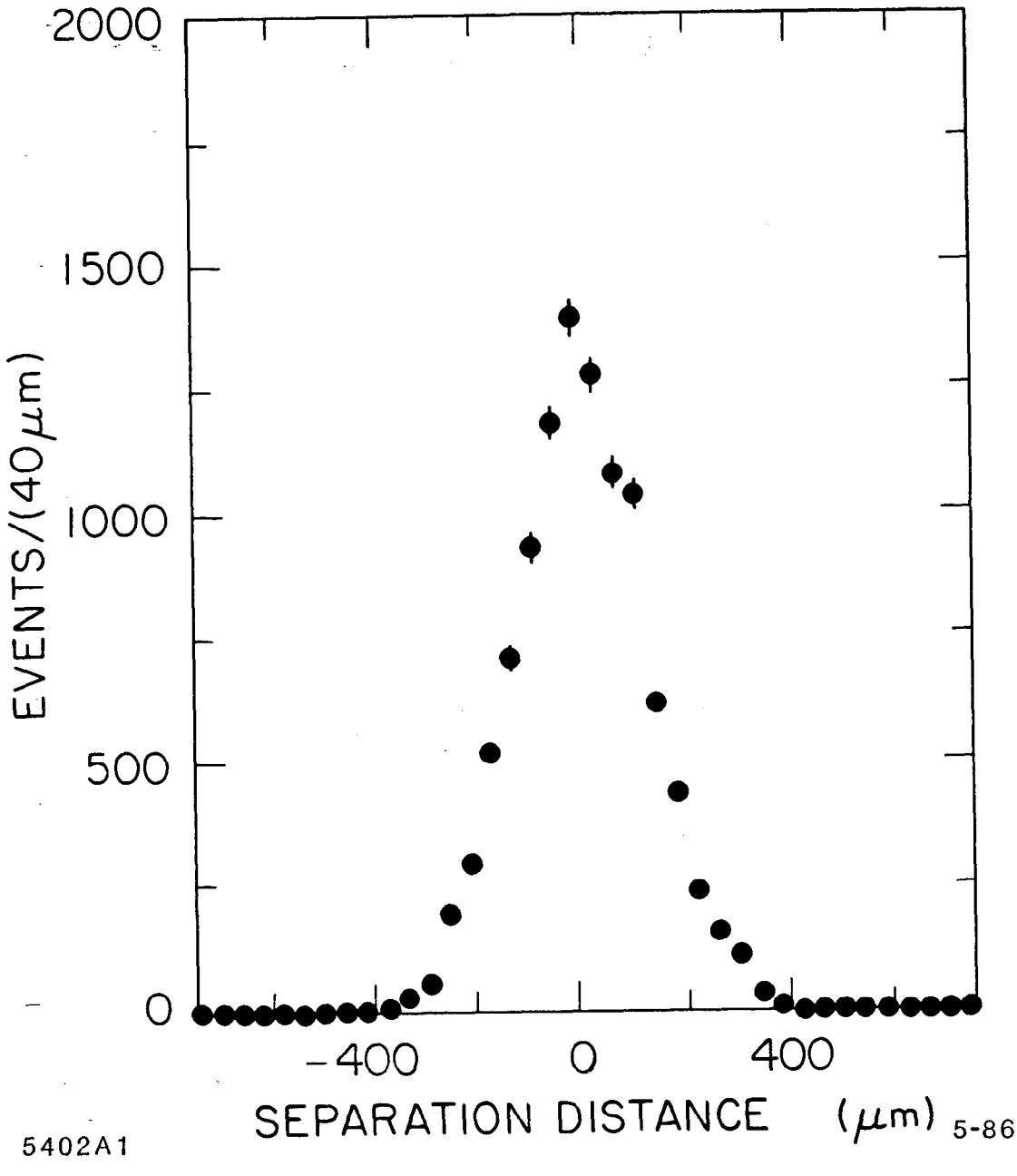
2000
1500
1000
500
0
EVENTS/(40μm)
-400
0
400
SEPARATION DISTANCE (μm)
5-86
5402A1

Fig. 1

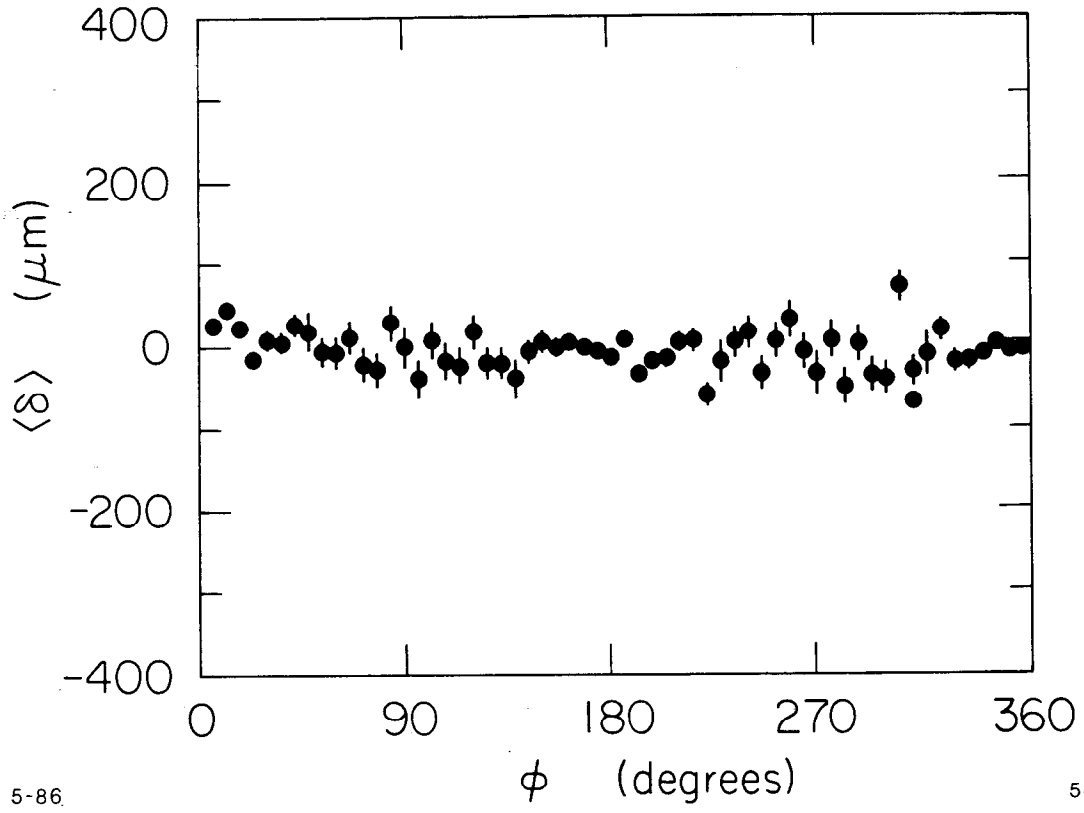

Fig. 2

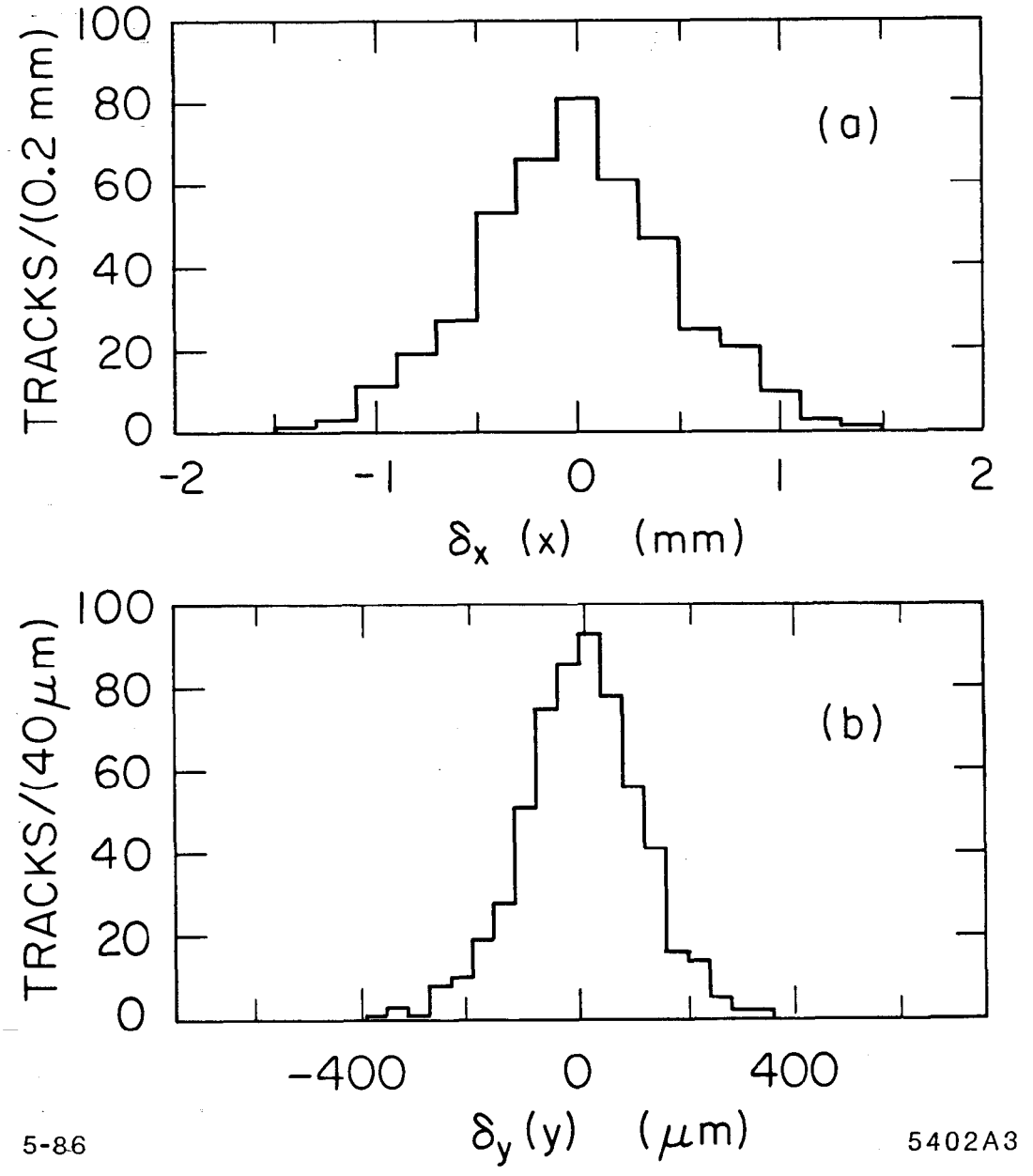
TRACKS/(0.2 mm)
100
80
60
40
20
0
(a)
-2
-1
0
1
2
δ_x (x) (mm)
TRACKS/(40 μm)
100
80
60
40
20
0
(b)
-400
0
400
δ_y (y) (μm)
5-86
5402A3

Fig. 3

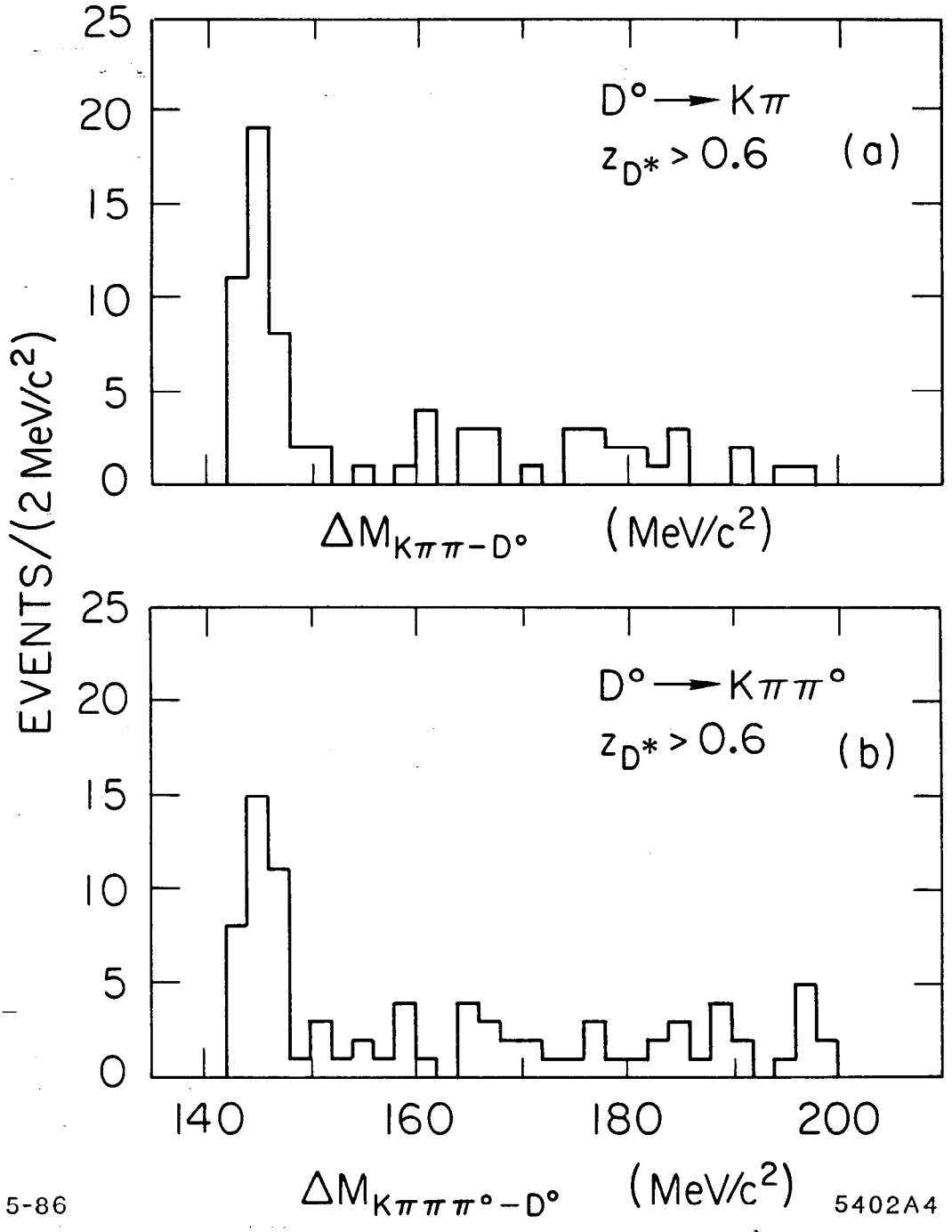
25
20
15
10
5
0
$D^0 \rightarrow K\pi$
$z_{D^*} > 0.6$
(a)
$\Delta M_{K\pi\pi - D^0}$ (MeV/c^2)
EVENTS/(2 MeV/c^2)
25
20
15
10
5
0
$D^0 \rightarrow K\pi\pi^0$
$z_{D^*} > 0.6$
(b)
140
160
180
200
$\Delta M_{K\pi\pi\pi^0 - D^0}$ (MeV/c^2)
5-86
5402A4

Fig. 4

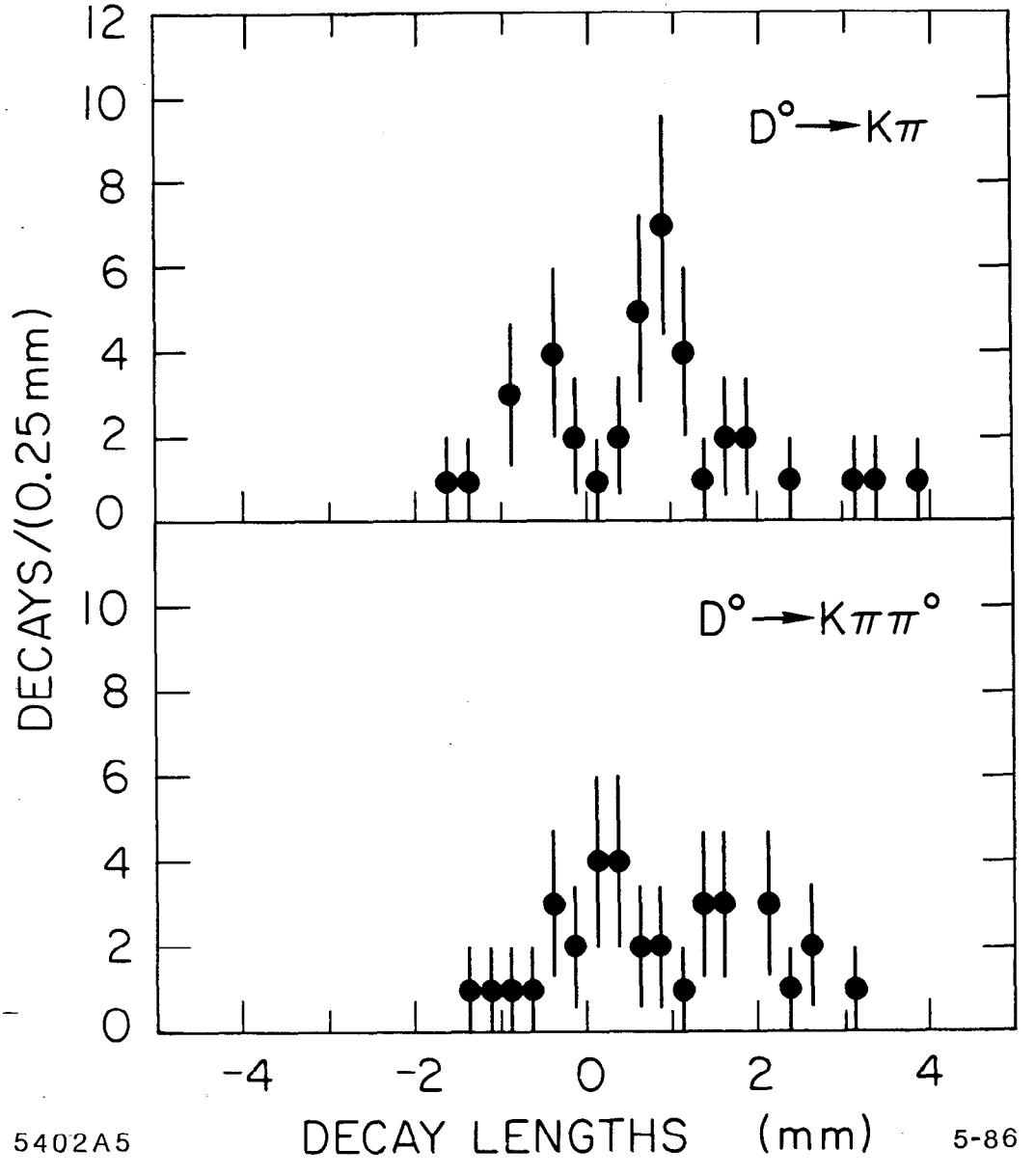
12
10
8
6
4
2
0
D°→Kπ
10
8
6
4
2
0
D°→Kππ°
DECAYS/(0.25mm)
-4
-2
0
2
4
DECAY LENGTHS (mm)
5402A5
5-86

Fig. 5

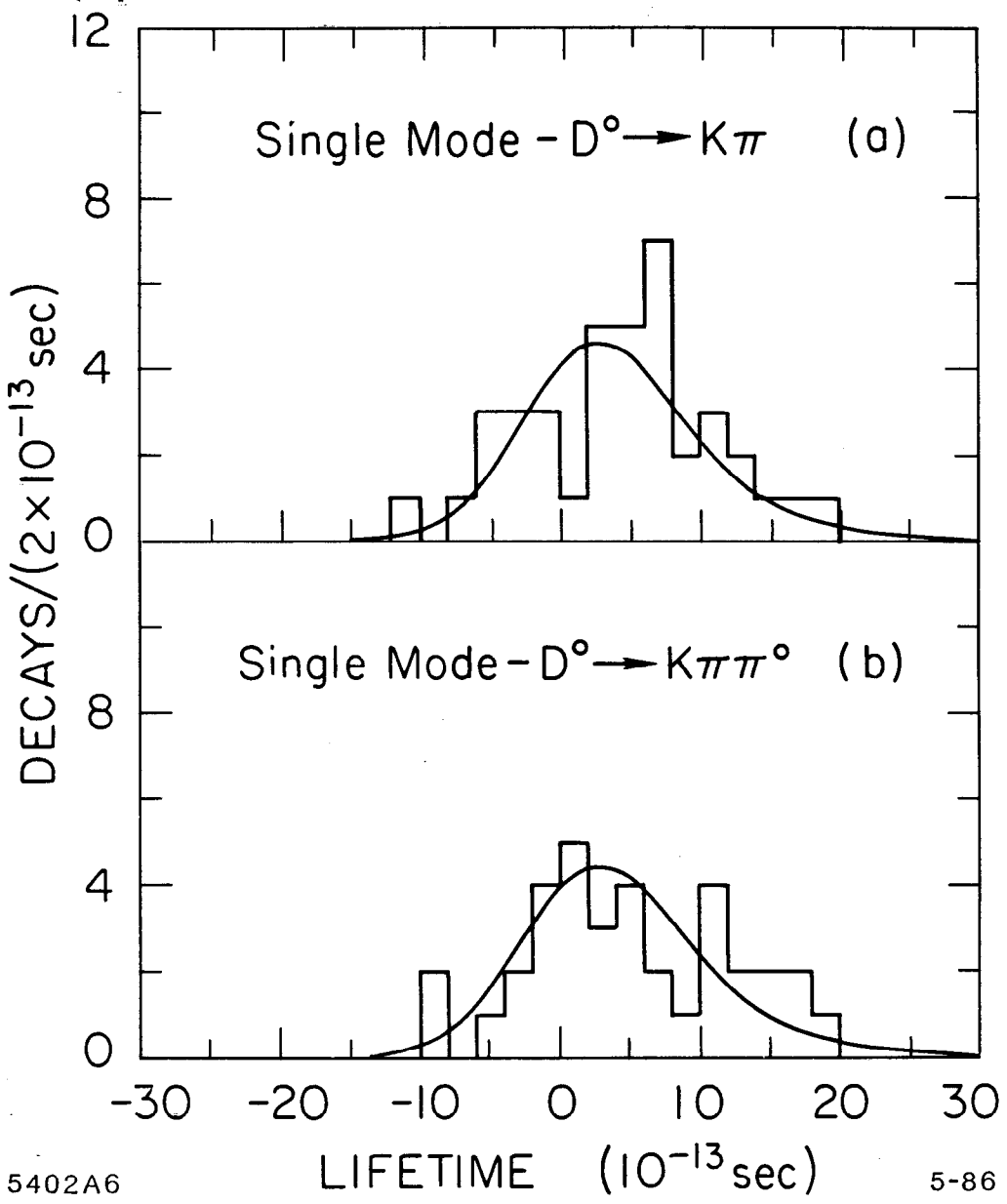
12
8
4
0
Single Mode - D° → Kπ (a)
DECAYS/(2×10⁻¹³ sec)
8
4
0
Single Mode - D° → Kππ° (b)
-30 -20 -10 0 10 20 30
LIFETIME (10⁻¹³ sec)
5402A6
5-86

Fig. 6

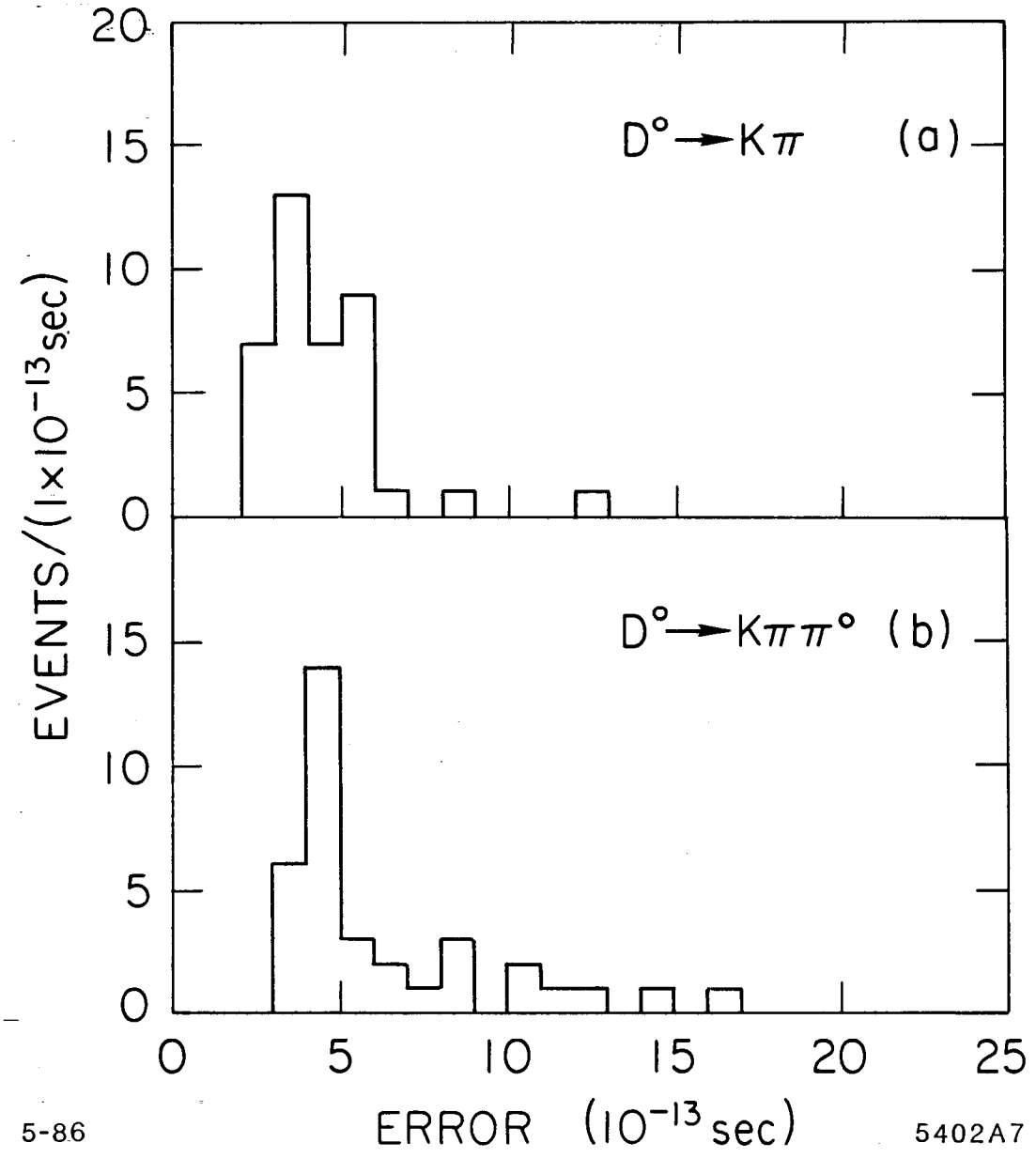
20
15
10
5
0
D°→Kπ (a)
EVENTS/(1×10⁻¹³sec)
D°→Kππ° (b)
0
5
10
15
20
25
ERROR (10⁻¹³ sec)
5-86
5402A7

Fig. 7

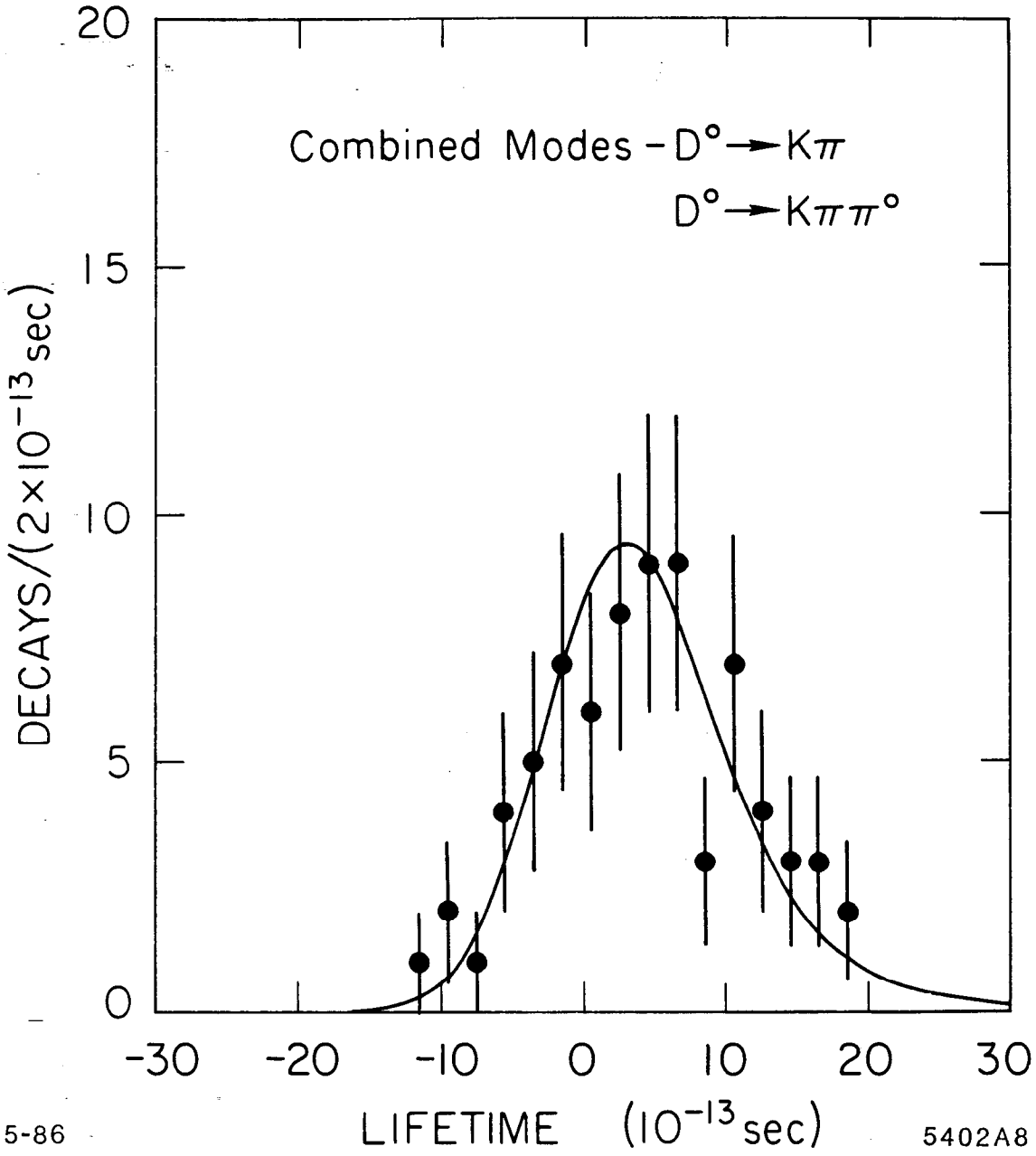
Combined Modes - D° → Kπ
D° → Kππ°
DECAYS/(2×10⁻¹³ sec)
20
15
10
5
0
-30
-20
-10
0
10
20
30
LIFETIME (10⁻¹³ sec)
5-86
5402A8

Fig. 8

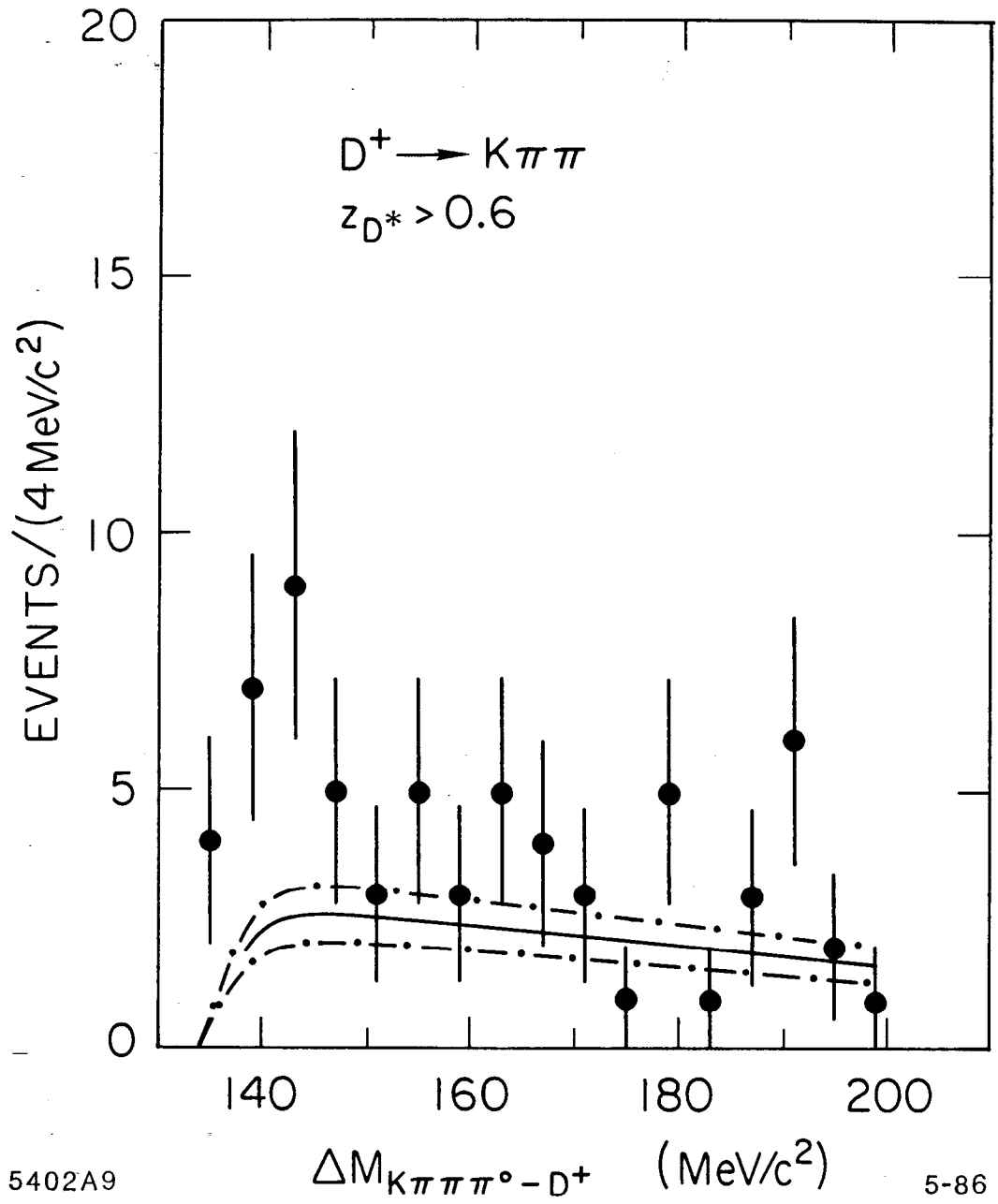
20
15
10
5
0
$D^+ \longrightarrow K\pi\pi$
$z_{D^*} > 0.6$
EVENTS/(4 MeV/c²)
140
160
180
200
$\Delta M_{K\pi\pi\pi^0 - D^+}$ (MeV/c²)
5402A9
5-86

Fig. 9

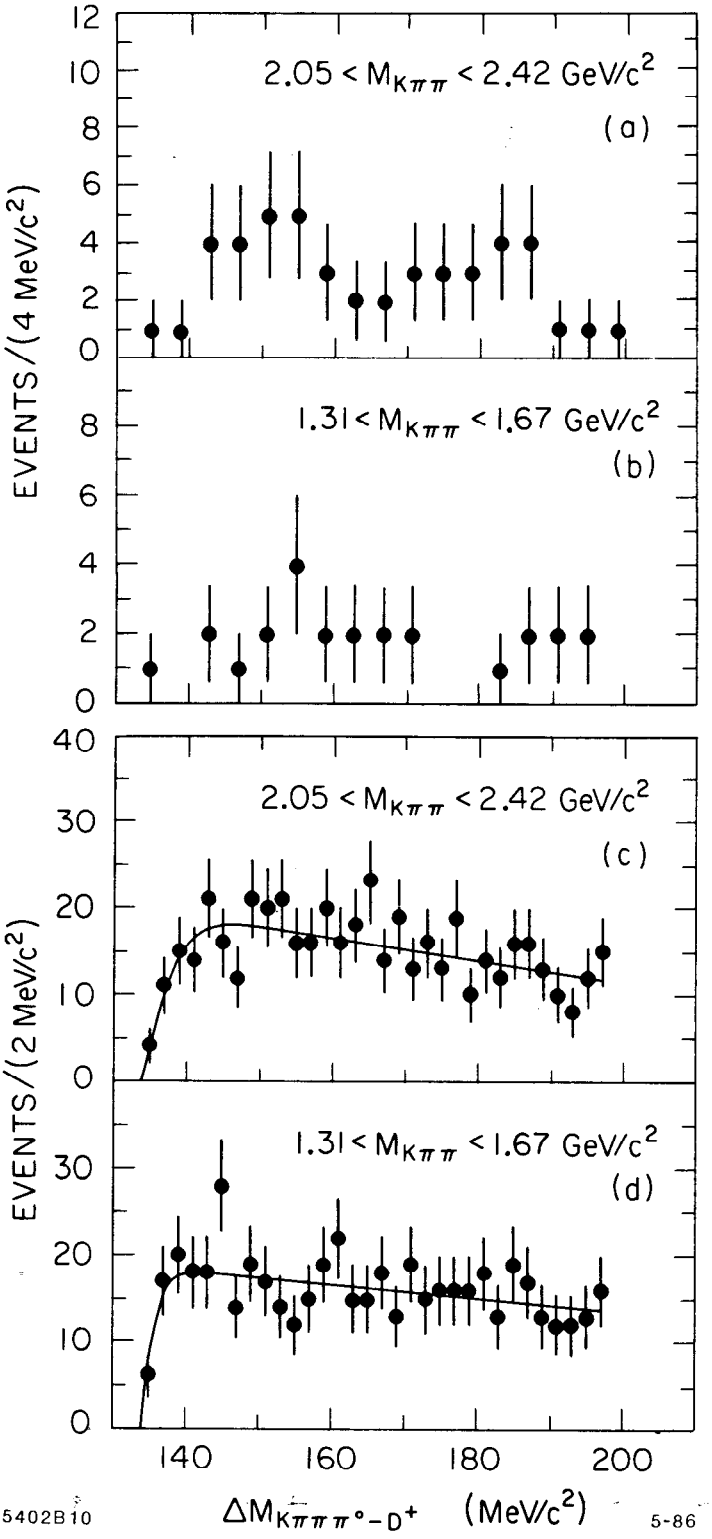
2.05 < $M_{K\pi\pi}$ < 2.42 GeV/c^2
(a)
1.31 < $M_{K\pi\pi}$ < 1.67 GeV/c^2
(b)
2.05 < $M_{K\pi\pi}$ < 2.42 GeV/c^2
(c)
1.31 < $M_{K\pi\pi}$ < 1.67 GeV/c^2
(d)
EVENTS/(4 MeV/c^2)
EVENTS/(2 MeV/c^2)
$\Delta M_{K\pi\pi\pi^0-D^+}$ (MeV/c^2)
5402B10
5-86

Fig. 10

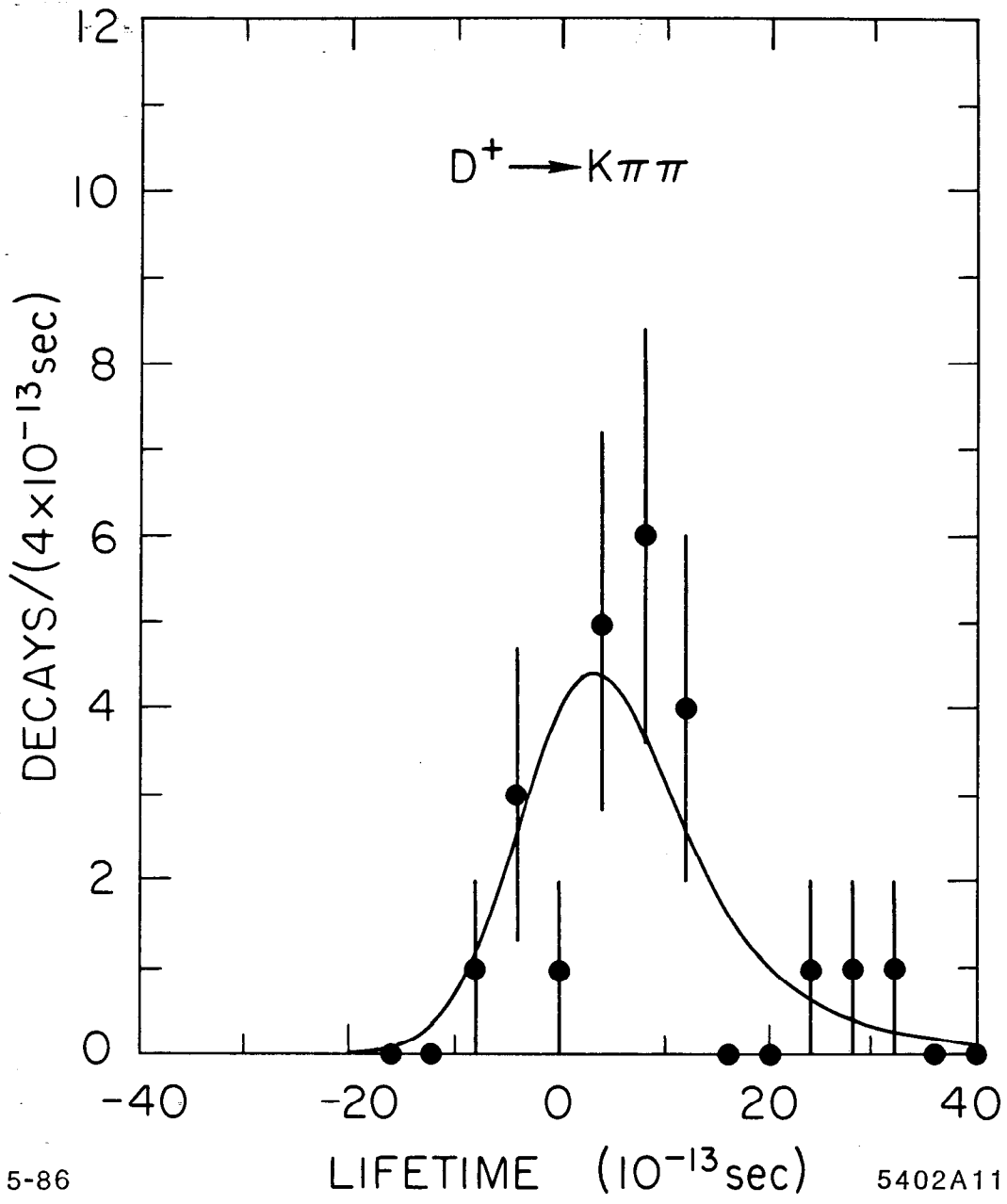
$D^+ \rightarrow K\pi\pi$
DECAYS/(4×10^{-13}sec)
0
2
4
6
8
10
12
-40
-20
0
20
40
LIFETIME (10^{-13}sec)
5-86
5402A11

Fig. 11

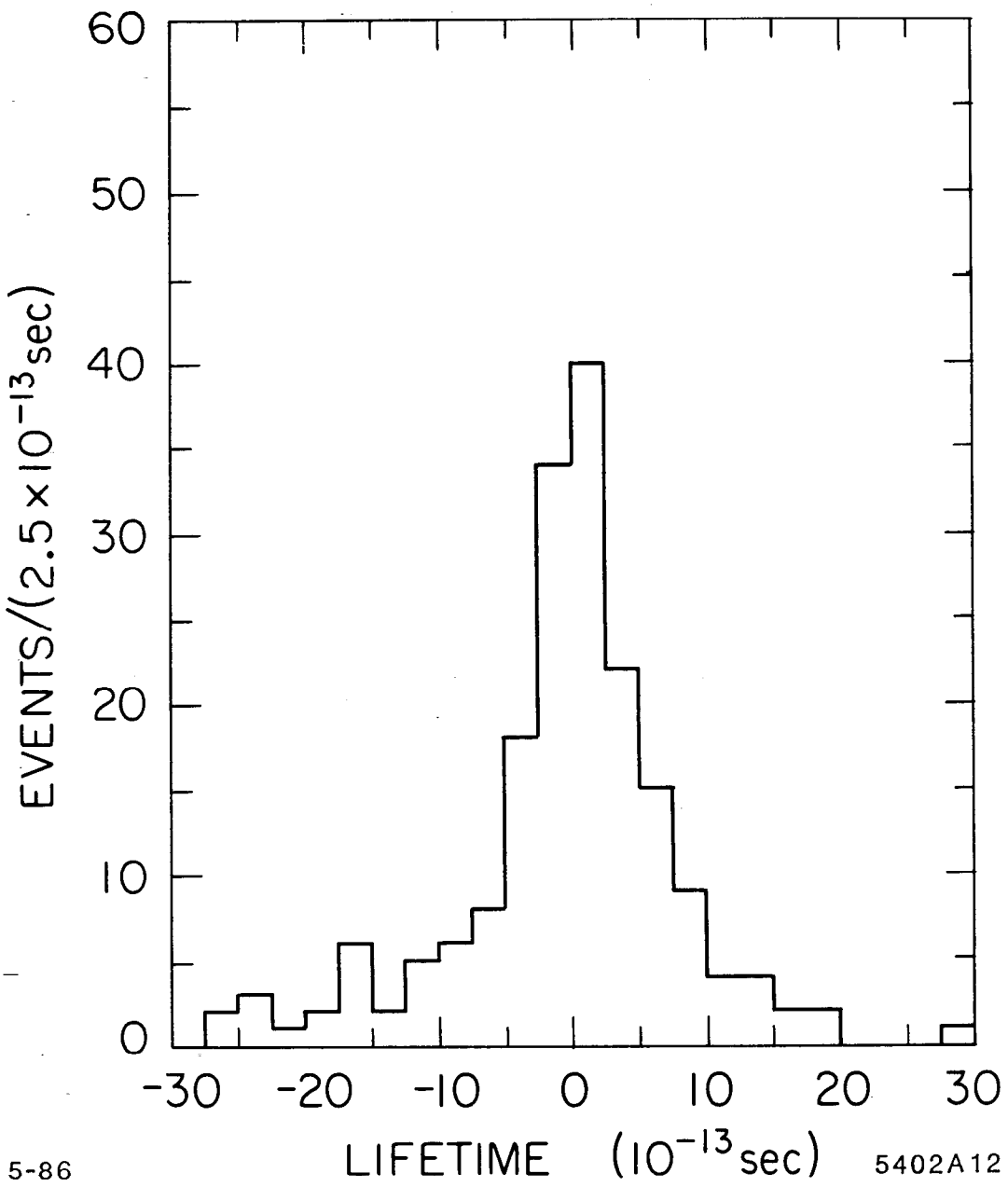
60
50
40
30
20
10
0
EVENTS/(2.5 x 10^-13 sec)
-30
-20
-10
0
10
20
30
LIFETIME (10^-13 sec)
5-86
5402A12

Fig. 12

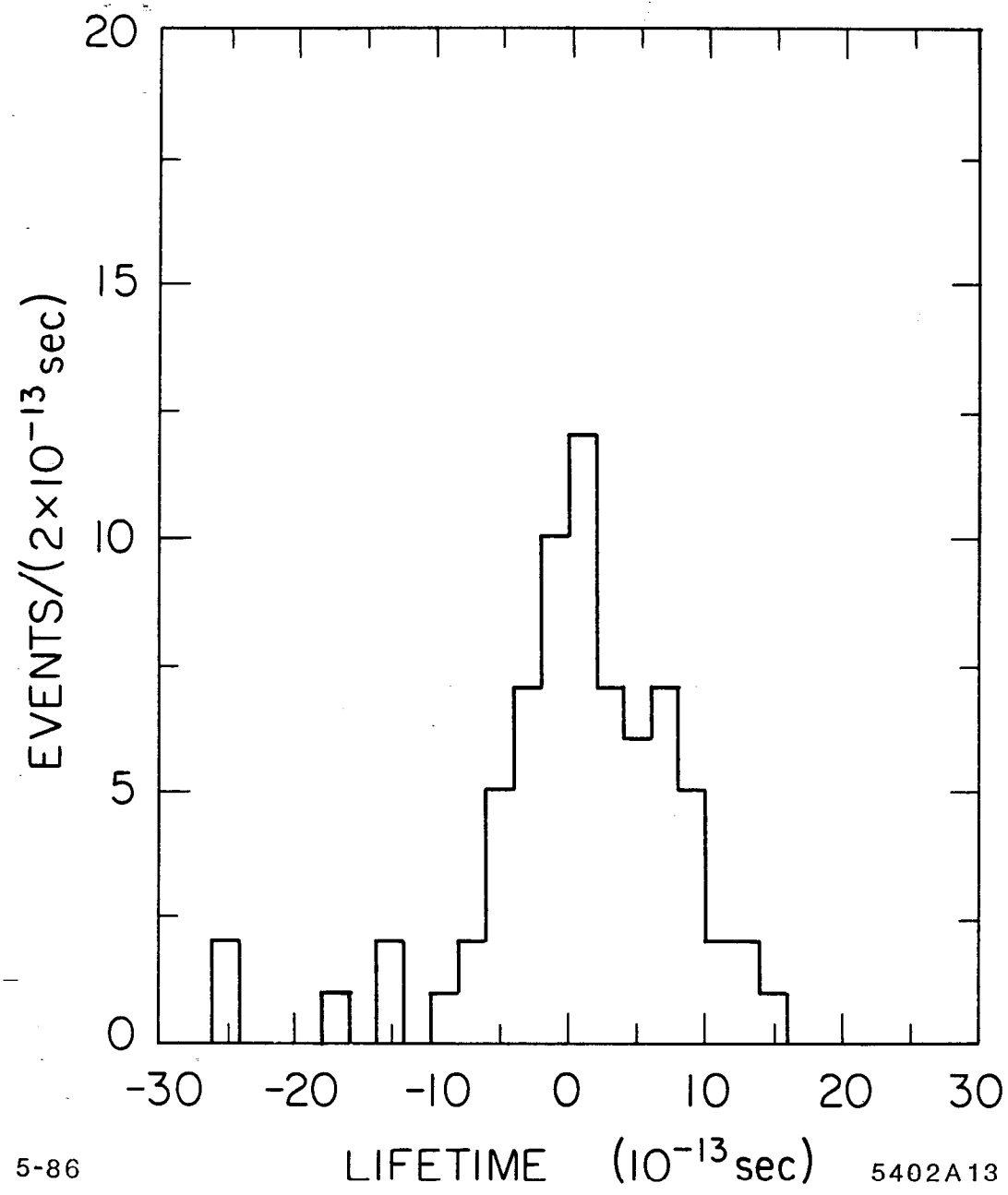
20
15
10
5
0
EVENTS/(2×10⁻¹³ sec)
-30
-20
-10
0
10
20
30
LIFETIME (10⁻¹³ sec)
5-86
5402A13

Fig. 13